NEW LAWS OF GALAXY KINEMATICS: CHALLENGES TO THE DARK MATTER PARADIGM

by

FRANCIS DUEY

A THESIS

Presented to the Department of Physics
and the Robert D. Clark Honors College
in partial fulfillment of the requirements for the degree of
Bachelor of Science

June 2023

An Abstract of the Thesis of

Francis Duey for the degree of Bachelor of Science
in the Department of Physics to be taken June 2023

Title: New Laws of Galaxy Kinematics: Challenges to the Dark Matter Paradigm

Approved: *James Schombert, Ph.D.*
Primary Thesis Advisor

Arguably one of the most controversial topics in cosmology today is that of the "missing mass problem". Today, there are two main competing theories that aim to address this issue: Cold Dark Matter (CDM) and Modified Newtonian Dynamics (MOND). The goal of this thesis is to directly address this issue by investigating the relationship between the visible mass of a galaxy, with its dynamical mass. A direct comparison can be made using what is referred to as the baryonic Tully-Fisher Relation (bTFR). In this thesis, we present the *new* WISE baryonic Tully-Fisher Relation for the Spitzer Photometry and Accurate Rotation Curves (SPARC) galaxy sample. This sample contains galaxies with improved photometry, new M/L models, and extended gas masses. An initial plot contains 62 redshift-independent galaxies whose distances were determined from either Cepheid stars, tip of the red giant branch (TRGB) stars, or supernovae. This new bTFR has a resulting slope of 4.00 ± 0.09, in agreement with predictions from MOND, and in sharp tension with values predicted by CDM models. In addition, a secondary plot containing the full 154 SPARC galaxy sample will be fit with the results from the calibration plot using distances provided by the CosmicFlows database. This new plot provides an opportunity to deduce a value of Hubble's constant (H_0) using every galaxy with an accurate rotation curve by varying the expected total baryon mass until a minimal fit is obtained. Such an

experiment results in a value of H_0 of 74.8 ± 1.8 (stat) ±1.5 (sys). This is especially important in context of what is known as the “Hubble tension” and leads to a statistically sound method of deducing an important constant in the MOND framework: a_0. All these results and the heavy implications of such will be discussed in earnest throughout this thesis.

Acknowledgements

I would like to thank the Spitzer Photometry and Accurate Rotation Curves (SPARC) team for providing the data necessary to complete this thesis. Additionally, acknowledgement should be made to the NASA missions that provided the Spitzer and WISE space telescopes whose archival image data was used for this project. Celestial data for the archived images was provided by the NASA/IPAC Extragalactic Database (NED). I would also like to thank my CHC Thesis Committee which includes Dr. James Schombert, Dr. Carol Paty, and Dr. Scott Fisher. In particular, Dr. James Schombert served not only as my primary thesis advisor, but also as my research advisor, academic and personal mentor, and the primary reason I was able to pursue such a fantastic subject for my future career. Along with this, Sara Tosi should also be acknowledged not only as a wonderful research partner, but close friend and confidant. I could not have completed this project without her constant support and advice. I want to.extend a special thanks my family for their undying encouragement throughout this arduous process.

I would also like take this opportunity to express my deepest gratitude to two extraordinary individuals who have played an invaluable role in my undergraduate experience. First and foremost, I would like to acknowledge the unwavering support and love of my best friend, Alexis Isaac. Her constant belief in my potential, infectious enthusiasm, and dedication to my success have been a driving source behind my perseverance. Alexis was present for every stress-induced late night practice session without complaint. Her warmth, kindness, and uncompromising support have made a profound impact on both my academic and personal growth. Alexis, your friendship has demonstrated the true meaning of unconditional love and

acceptance. I will forever be thankful for the time we have spent together, and the time we have yet to experience.

Finally, I want to express my appreciation for an individual who has also had an immeasurable impact on my life throughout these past four years, Felix Gladwell. Felix, your presence in my life has been a gift I cherish deeply. Beyond being a friend, you have become a confidant and trusted source of advice and support. Your kindness, humor, and unique ability to make any situation unserious has provided me with a much-needed sense of lightness and perspective. Whether or not you meant to, you have pushed me to embrace new experiences and reminded me of the importance of living in the present moment. Your unwavering friendship and genuine care has made a lasting impact, and I am incredibly fortunate to have you by my side. Thank you for being the person who has brought so much laughter and joy into my life. I am grateful beyond words.

Table of Contents

List of Figures

List of Tables

Introduction

If there was ever a perfectly elegant way to describe the Universe, physics is it. Even the most intricate interactions can be broken down into logical, rule-abiding relationships that help explain how and why a system works. While physics has consistently served as an excellent descriptor for the immediate world, there is a great deal of uncertainty at larger scales. This becomes evident when considering the study of the origin and evolution of the Universe; better known as cosmology. In the past, the lack of understanding was simply a product of limited technology. With the introduction of improved infrared telescopes, computing power, and a general advancement in our collective scientific knowledge, this is no longer the case. In fact, the past 10 years of cosmological research have accelerated the ways in which we can study both the local and non-local Universe. One of the most critical of these, the dark matter or "missing mass" problem, has been of primary concern thanks to new galaxy kinematic data that has allowed researchers to readdress this paramount issue. Our understanding of everything in the Universe may very well depend on this issue. The dark matter problem, which will be addressed in depth throughout this paper, ties into our understanding of the least understood of the four fundamental forces in our Universe: gravity. Gravity makes up the very fabric of the universe, making our understanding of it paramount for a progressive framework of cosmology to prevail.

This paper will be directly addressing the dark matter problem. Combined archived images from two NASA space telescopes (Spitzer and WISE) have been used to produce multi-color aperture photometry of 154 gas-rich spiral and dwarf galaxies that make up the galaxy sample used for this paper. Using this sample's known rotation curves, the dynamical mass of these galaxies will be obtained. Also, galaxy surface photometry will be used with stellar population models to obtain the baryonic mass of the same galaxies. The comparison of these

mass models will help to determine if dark matter theory, which under current cosmological models is heavily reliant on gravity, is accurate. If not, this may change our understanding of matter interaction at certain accelerations and help answer some age-old questions about the Universe.

Chapter 1: Literature Review

Dark Matter

Dark matter has been in the minds of astronomers for decades. The idea started to gain significant traction starting in the 1930s with the observations made by Swiss American astronomer Fritz Zwicky. While observing what is known today as the Coma Cluster, Zwicky observed there was simply not enough luminous mass in the galaxies to explain the velocities at which they were moving (Zwicky 1933). Namely, there was a discrepancy between the velocity dispersion of the cluster with its luminous mass. A logical conclusion was then made that the mass is there, but it is *not* luminous. The popularity of this idea was accelerated in the 1970s when Vera Rubin and William Ford began observing the kinematics of individual galaxies (Rubin & Ford 1980). More specifically, the rotation curves of these galaxies. Using optical observations of hydrogen-alpha (Hα) emission lines, they were able to plot the rotational velocity as a function of radius. The researchers were shocked to see that the plots seemingly violated Kepler's third law, which states that the square of a planet's orbit is proportional to the cube of its radius. Under this assumption, the rotational velocity of a galaxy should decrease as you get further from the galaxy's center. Instead, it was seen that the rotation curves asymptotically increased with radius, eventually reaching a constant value. At this point, astronomers were still convinced that these rotation curves would eventually fall at larger radii as measurements at the time ranged between only 10-20 kiloparsecs. The addition of radio telescopes in the 1980s, however, killed this assumption (Bosma 1981). Neutral-hydrogen 21-cm emission lines demonstrated that the rotation curves of galaxies extended for hundreds of kiloparsecs. With Newton's Law of Gravity in mind, these observations imply there is a significant amount of mass in the outer regions of galaxies. The hypothetical regions of unseen

matter distributed around a galaxy (gravitationally binding the matter in galaxies), became to be referred to as dark matter halos. With growing interest in dark matter to answer cosmological questions, theory shifted towards what exactly the invisible mass could be made of.

When Zwicky first postulated that there must be this invisible mass in our Universe, the scientific community was rather hesitant to propose the idea that mass was made out of anything not already in the Universe (de Vaucouleurs 1960). As such, baryonic candidates were among the first contenders for the aptly named "dark matter". The first candidates consisted of low-mass, faint stars, but were quickly ruled out due to the high star formation rates needed for this to occur (Faber & Gallagher 1979). Overall, it was very difficult for astronomers to reconcile with already well-established star formation scenarios. The non-luminous counterparts to these low-mass stars were also quickly eliminated as possible solutions for the missing mass. These objects, ranging from rocks and planets to brown dwarfs, would need to be in vastly high numbers. Once the technology was developed to observe such objects, it was quickly seen that there were not nearly enough of these objects. Astronomers then shifted gear and turned their hope to high-mass, non-luminous objects. This category, better known as MACHOs (MAssive Compact Halo Objects) consists of things such as white dwarfs, neutron stars, and black holes. Dense by definition, these objects have an incredible gravitational pull on the objects around them. It thus made sense for there to simply be a large number of these items that allow for the fast rotational velocities of galaxies. Unfortunately, for this to be true, several already accepted facts about our Universe would need to be challenged or altogether ignored. One of the biggest issues was the time it would take for such a number of these objects to form. This is due to *how* such objects are formed. When a massive star goes supernova (runs out of fuel and collapses), every proton and electron is crushed into neutrons. If the star had a high enough mass, this

process would cause the star to collapse into a black hole. While simple enough in explanation, the timescale for such a process would require the Universe to be thousands of times older than what has been observed. Additionally, this process would require 90% of all stars to go supernova, something astronomers would easily see. The emergence of gravitational microlensing only reaffirmed the rejection of this hypothesis. It is a well-known fact that gravity bends light. When this occurs in space, objects with high mass (and thus strong gravitational pull) deflect the light from more distant sources such that the appearance of multiple images is made. If dark matter halos were made solely of MACHOs, this would be reflected in the microlensing of these objects. This was not seen, eliminating a 100% MACHO dark matter halo at the 95% confidence level (Alcock et al. 2000). All in all, the universe is too young and the sky is too dark for baryonic dark matter to be a viable solution.

This brings us to the state of dark matter research today. With baryonic dark matter eliminated as a possible solution, it was determined that if dark matter does exist, it must be made of something other than baryons and leptons (the elementary particles of the Universe). At first, the most compelling candidate for this is what is known as a neutrino (White, Frenk, & Davis 1983). Before knowing their mass, neutrinos matched all criteria required for dark matter. Invisible on the electromagnetic spectrum, electrically neutral, and only interacting with standard particles via the weak force, neutrinos were ideal. Unfortunately for the dark matter community, it was later discovered that neutrinos were simply too low in mass to have the desired gravitational pull (Olive et al. 2016). A conclusion was then made that if dark matter is a particle, it must reflect all characteristics of a neutrino, but have a much higher mass. Today, these mystery particles are referred to as “Weakly Interacting Massive Particles” or WIMPs for short. These particles, predicted to be about 100 times the size of a proton, will theoretically only

interact with matter through the weak force, one of the four fundamental forces governing the laws of physics (Jungman et al. 1996). Under the assumption these particles exist, two primary methods for their detection exist today: indirect detection via the cosmic microwave background (CMB) or particle accelerators, and direct detection via interactions with standard particles. In theory, by smashing two protons at incredible accelerations (giving them high energy), scientists could recreate a scenario similar to that of the Big Bang. The "missing" energy produced from colliding two standard particles would be direct evidence of dark matter. This is because doing so would break the standard model, opening up the idea for a new "dark" physics which would lead to the possibility of particles not in the standard model (WIMPs). These particle accelerators exist, costing around $5 billion to make and $1 billion annually to maintain. While no evidence of dark matter has resulted from these experiments, confirmation of the Higgs-boson particle was a tremendous feat. This discovery completed the standard model of physics but additionally closed the door for this particle to be dark matter. The lack of progress made in this search, however, has many in the scientific community questioning if the time, energy, and money required to keep the accelerators running is worth their continued existence.

On the other side of the particle detection program, is the direct observation of dark matter interacting with a known particle. The process of which also takes place deep underground using massive containers. The innermost portion of these tanks is a container filled with xenon (Aprile et al, 2023). Surrounding this is a second tank with gamma-ray absorbing liquid. The outermost tank envelopes the previous two, holding up to 70,000 gallons of pure water. These tanks are then placed about a mile underground to prevent false alarms from radioactive particles in the Earth's atmosphere interacting with the xenon. The goal of such a setup is to directly observe the energy transfer that would theoretically occur if dark matter were

to pass through any of the xenon particles. As the dark matter bumps the nucleus of the xenon particle, both light and an electrical charge would be given off. Both of these would be easily detectable and confirm the existence of dark matter. In the 40 years from their first appearance, however, no detection has been made.

While particle detection has been a popular area of study, numerical simulations hold just as much attraction in the dark matter community. The 1970s produced a litany of scientific advancements. One such advancement was the ability to simulate the evolution and kinematics of galaxies (Ostriker & Peebles 1973). Today, there are two main objectives the dark matter community hopes to gain from these simulations: 1) large-scale cosmological structure predictions and 2) dark matter halo shapes (White & Rees 1978). The former was wildly popular when this technology first emerged (Blumenthal et al. 1983). In part, this was because the debate on whether or not dark matter was relativistic or non-relativistic (hot or cold) had yet to be resolved (White, Frenk, & Davis 1983). This debate was vital, as the answer to this drastically changes how large-scale cosmological structures formed in the early universe. With the addition of redshift surveys, a conclusion was made that dark matter must be cold (Peebles 1982). When running simulations under the assumption dark matter is relativistic, it was apparent that the cosmic filament structure seen today contrasts with those produced via simulation. On the other hand, these structures could occur should the dark matter be non-relativistic (i.e. cold). The timeline of when these structures began to form was also only reasonable under the latter condition. As such, the "hot dark matter" theory faded in popularity. Numerical simulations today have strayed from the cosmological scale, focusing primarily on the structure of dark matter halos in galaxies. This first came about with observations made in the 1980s. Early simulations in this time focused on disk galaxies and almost immediately ran into an issue. Basic

laws of physics in a Newtonian regime indicate that as time passes, disk galaxies should collapse from a thin, flattened structure to a more spherical one (Ostriker & Peebles 1973). As the stars and gas of a disk galaxy interact with one another, the galaxy will lose energy. A lack of a counteractive force would cause the disk galaxy to become unstable and eventually collapse in on itself. This point is where dark matter halos really began to gain popularity in the astrophysics community. Adding these large structures to the evolutionary simulations resulted in stable disk galaxies as seen today. Unfortunately, while dark matter halos do solve a large-scale stability problem, several small-scale issues arise under this assumption. One such issue is commonly referred to as the "Cusp-Core Problem" (de Blok 2009). Under cold dark matter (CDM) theory, dark matter halos should have a density profile that rises steeply near its center, forming a "cusp". Observations of dwarf galaxies, however, illustrate the contrary. Uniform density profiles are instead surveyed; a problem that the CDM model has yet to reconcile with. A secondary, yet equally problematic issue with current dark matter models is the supposed diversity in the halos (Navarro et al. 2010). Dark matter models indicate that dark matter halos should be similar in structure and density profiles. Yet, when looking at the rotation curves of galaxies, it was seen that the density profiles vary greatly between galaxies. This issue points towards a baryon-dark matter connection and the first major challenge to the CDM framework (McGaugh 2014).

Today, dark matter halo simulations make up a majority of numerical simulations. The motivation for these requires a second look at the rotation curves of galaxies. After using N-body simulations to obtain the shape of a dark matter halo for certain galaxies, researchers will then scale these structures to match the rotation curves of these same galaxies (Li et al. 2019). Under the assumption dark matter exists, knowing the shape of a galaxy's dark matter halo would

provide crucial information to answer age-old questions of how galaxies behave. The evolutionary history of a galaxy, properties of dark matter, and how dark matter is distributed in a galaxy are all results researchers hope to gain from accurate models of dark matter halos. Serious issues arise, however, from this method of analysis.

Take what occurs when applying this method to spiral galaxies for instance. More commonly than not, massive discrepancies are seen in the rotation curves of galaxies being produced from these simulations and those directly observed such as in the spiral arms (Lelli 2022). As previously mentioned, these plots take the rotational velocity of a galaxy as a function of distance from the galaxy's center. Rotation curves are essential for understanding mass distribution and structure in a galaxy. Thus, numerical simulations must accurately reproduce what is being observed to have any sense of validity; something this area of research is frequently missing. A common response to this problem is to introduce several free parameters when it comes to the properties of the dark matter halos. Of these, the most common adjustments are to the density and scale length of the halo. These parameters are altered to fit the observed rotation curves of galaxies. Several issues are evident with this approach. For one, the general shape of the dark-halo fits (typically taking the form of $p(r) \propto C/(r/r_0)^{\alpha}$) is not deduced from predicted properties of dark matter, but instead a result of shapes from N-body simulations using a non-interacting particle possessing gravitational influence as the only direct interaction with baryons. This produces a generic profile shape which can then be scaled to high/low densities or big/small scale sizes by changing density (p_0) with radius (R_c). Such an approach has a variety of issues, particularly with the evolution of dwarf galaxies. Success from these simulations ends when trying to scale up to large spiral galaxies as a result of inconsistent surface densities. The response to this is typically tweaking simulations until there is a match to what is being

observed. Put simply, building galaxies using ad hoc methodology. These shortcomings raise the discernible question of the need for the existence of alternative theories. In intense opposition to the dark matter community, a predictive set of theories known as MOdified Newtonian Dynamics (MOND) has provided a promising avenue.

Modified Newtonian Dynamics (MOND)

Both the rotation curves of disk galaxies and simulated dynamics of galaxies at low accelerations provided dead ends for dark matter cosmologists from the outset. Israeli astronomer and professor, Dr. Mordehei Milgrom, recognized these shortcomings and proposed an alternative solution in the 1980s. Representing an alternative approach to the missing mass problem, MOND "...posits a breakdown of Newton's law of gravity below a_0, after which the dependence with distance became linear" (Scarpa 2006). In other words, at a certain (and very low) acceleration, the gravitational force experienced by a star in a given galaxy is proportional to the square of its centripetal force. This is in opposition to the centripetal acceleration proposed by Newton's second law. Hence, this theory is given the name Modified Newtonian Dynamics. While not complete under relativistic circumstances, MOND provides a tight and testable answer to the missing mass problem in galaxies. To understand the foundations for the MOND theory, attention needs to be placed back on one of the main issues of dark matter theory: rotation curves.

A primary issue of rotation curves for many comes from an inconsistency in mass profiles. Mass values obtained through stellar population models of galaxies (producing mass-to-light (M/L) ratios in the stellar disks) often do not match the mass values derived from the rotation curves and Newton's law of gravity. Fortunately for MOND, the breakdown of Newtonian dynamics solves this issue without the addition of dark matter. Arguably the most

important characteristic of the MOND theory is that at very low accelerations, the Newtonian force law adds a constant a_0 to the force $g = 9.8\ m/s^2$ such that acceleration goes as $\sqrt{(ga_0.)}$ This relation came about when Milgrom considered the possibility that "in the limit of small accelerations, the inertia force is not always proportional to the acceleration" (Milgrom 1982). Assuming this new relation results in the inertial force becoming quadratic, producing an asymptotic velocity that gives the same asymptotic shape of galaxy rotation curves at large distances. Not only does this provide an explanation for rotation curves without the addition of dark matter, but makes specific predictions that are easily testable and result in a potentially falsifiable theory. Dwarf galaxies in particular provide a strong test environment for this assumption of MOND due to their low stellar densities implying slow accelerations. Since the MOND regime involves such accelerations, studying the kinematics of these particular galaxies allows for ample opportunity for MOND skeptics to falsify the theory. As of today, no such falsification has occurred.

It is no secret that rotation curve fitting using dark-halo fits does in fact work. As previously mentioned, however, this is usually accomplished with the use of three free parameters (halo mass, halo density, and galaxy disk mass). Sharply contrasting this approach, is that of MOND. The only free parameter used in MOND for fitting rotation curves is the M/L value for the disk of the galaxy. This value is important as stellar mass measurements are a result of adding together the luminosity and M/L values. Adding this to the gas mass (found via HI flux) results in the baryonic mass of a galaxy. MOND uses only the baryon mass distribution to predict galaxy motion, making these values all the more significant. Under the assumption that a_0 is a constant value, and Newtonian dynamics break down at this value, rotation curves can be derived strictly from the baryons; a sharp contrast to dark-halo fits. As early as 1990, it was seen

that “MOND rotation curves derived from the observed stellar and gaseous mass distribution agree with the observed rotation curves as well as, and in some cases better than, three-parameter dark-halo models” (Begeman et al. 1990). The sample used in this paper consisted of spiral galaxies, showing that although dwarf galaxies provide excellent tests for MOND accuracy, this one-parameter approach applies to more than one galaxy type. In fact, the rotation curves of a myriad of galaxy types and sizes have been accurately fitted using MOND since this initial study.

The predictive and simplistic nature of MOND has been an attractive characteristic of the theory for many in the community. Milgrom’s earliest papers identified seven key predictions. Of these, the following five of which are most prudent to this analysis and have yet to be falsified:

1. Velocity curves calculated with the modified dynamics based on the observed mass in galaxies should agree with the observed ones.
2. The relation between the asymptotic velocity (V_{flat}) and the mass of the galaxy (M)($V_{inf}^4 = MGa_0$) is an absolute one.
3. Effects of modified dynamics are predicted to be particularly strong in dwarf galaxies.
4. Disk galaxies with low surface brightness provide particularly strong tests [for MOND].
5. There is an expectation that there is a “correlation between the value of the average surface density (or brightness) of a galaxy and the steepness with which the rotational velocity rises to its asymptotic value”. In other words, the lower the surface density, the more shallow (and slower) rise in velocity (McGaugh 2020).

Prediction 1 remains accurate via ongoing rotation curve fitting and leads into the expectations outlined by predictions 3 and 4. While these predictions are important, it is predictions 2 and 5 that carry heavy implications for the most recent publications made in this area of research. Concerning prediction 5, it is important to pay close attention to the wording provided by Milgrom. Once again, this requires a visit back to the rotation curves of galaxies as

relating the surface density of a galaxy to the steepness of its rotational velocity has great significance. Recall that rotation curves take a galaxy's rotational velocity as a function of the galaxy's radius from its center. In other words, a rotation curve shows the individual velocities of the stars and gas of a galaxy as they orbit at different radii about the galaxy's center. Thus, it can be determined from these curves how much of a galaxy's mass is contained at a certain radius.

The relationship of $V_{inf}^4 = MGa_0$ (as provided by prediction 2) is a core tenant of MOND theory. Not only does it include the modified version of gravity, but also has a predictive power when analyzing the relationship between the baryonic mass (stars and gas) of a galaxy with its dynamical mass. This relationship is referred to as the baryonic Tully-Fisher Relation (bTFR) and will be discussed in earnest in the following section. From the bTFR, there is an additional opportunity to measure the constant a_0 directly from observational data. Defining this value is vital for analysis under a MOND framework, underlying the ambition to do so.

Under the classical assumption of Newtonian dynamics (CDM theory), the observed rotation curves cannot exist without the addition of dark matter. Milgrom had an alternative theory, as outlined in prediction 5. Should Newtonian dynamics break down at a certain acceleration (a_0), we should see that the distribution of mass in a galaxy heavily influences the shape of its rotation curve. This exact relation is seen in the rotation curves of a variety of galaxy types, sizes, and luminosities. A valid conclusion can be drawn from this: it is not dark matter, but baryons that drive the motion of a galaxy. This idea is further supported by what is now referred to as "Renzo's Rule" which states that "for any feature in the luminosity profile there is a corresponding feature in the rotation curve and vice versa" (Sancisi 2004). This idea comes from observations that there are "bumps" in the luminosity profile of galaxies (such as spiral arms) that are reflected in the rotation curve. It is impossible to explain these so-called bumps

and wiggles of a galaxy's rotation curve with dark matter alone. The influence of the visible mass of a galaxy on its dynamics once again dark matter-baryon connection outside gravitational forces. While this influence is more prevalent at smaller radii, it is nevertheless a challenge to the current CDM theory that has yet to be resolved.

Arguably one of the most important consequences of MOND's predictive nature is the emergence of the Tully-Fisher relation as yet another test of a dark matter-baryon connection. Distance measurements to distant objects have always been a challenge for astronomers. In 1922, Ernst Opik used the virial theorem to determine the distance to the Andromeda galaxy. Relating the total kinetic energy of a self-gravitating body as a result of its moving parts, this theorem is often the root of many scaling relations. Its ability to relate two observable properties of galaxies (velocity dispersion and effective half-light radius) to their unobservable quantity (mass) makes this theorem a powerful tool in astrophysics (Swinburne University). This theorem was a popular method to conduct distance measurements up until the 1970s when Dr. Richard Tully and Dr. James Fisher proposed a new relationship from their study of spiral galaxies. Under the expectation that more massive galaxies would not only be more luminous but rotate faster, the pair presented what is known today as the Tully-Fisher relation (Tully & Fisher 1977). This relation is an empirical power-law relationship between the luminosity of a galaxy (L) and its rotational velocity (v) represented as $L \propto v^{\alpha}$ (NASA/IPAC 2023). The power of this relationship cannot be understated. Not only did it allow for significant progress in extragalactic distance scales, but also brought about a major challenge for the dark matter community: a clear relationship between the mass and luminosity of a galaxy. Initially, this relationship was welcomed by the dark matter community. A general assumption made by CDM theory is that if one were to theoretically take a scoop of the universe to construct a galaxy, the result would be a

mix of dark matter and baryons. This relationship is represented as L α V^{α}. Essentially, one would expect an increase in gravity (V) with increased mass, even if most of the mass is invisible. Deviating from this assumption and Opik's virial theorem, the Tully-Fisher relation instead demonstrated a universal mass-to-light ratio (M/L) for all galaxies. Doing so was significant as now the luminosity of a galaxy could be used as a proxy for its mass. Considering the assumption that dark matter dominates the mass of galaxies, this result was anything but expected. The additional fact that scatter on the plot was minimal also brings into question a connection between dark matter and baryons; a result in sharp contrast to CDM theory.

While the Tully-Fisher relationship had been well established, it did not come without some limitations. In its original form, the Tully-Fisher relation addressed bright galaxies and concluded that brighter galaxies tend to have steeper rotation curves. These galaxies are stellar-dominated, eliminating the need to measure the mass of the galaxy's gas component. The lack of the galaxy's baryonic mass became a problem once low-mass (gas-rich) galaxies were added to the Tully-Fisher relation. Once done, it was seen that the tight, linear fit drastically deviated as the low-mass, gas-rich galaxies fell well below the Tully-Fisher relation. It was then proposed in the 1990s by astronomer Stacy McGaugh that considering the baryonic mass of a galaxy (mass of the stars, gas, and dust) as opposed to the stellar mass would result in a more accurate correlation between a galaxy's mass and its rotational velocity. The results of this hypothesis speak for themselves. Once the baryonic mass of galaxies was accounted for, the linearity of the Tully-Fisher relation was restored (McGaugh et al. 2000). This relation is now referred to as the baryonic Tully-Fisher Relation (bTFR) and is a well-established method in observational cosmology for the analysis of galaxy mass and its evolution over time.

The restoration of linearity in the Tully-Fisher relation brought about another striking result. When the baryonic mass was accounted for, the slope of the resulting relation became shallower. The debate surrounding this slope is ongoing today but has been determined to lie in the range of 3-4 depending on how the luminosities and rotational parameters of analysis are defined (Lelli et al. 2019). This implies that the rotational velocity increases with the third or fourth power of the baryonic mass. McGaugh's estimate, lying on the higher side of this relation, made the connection of this power relationship to that outlined by MOND. The significance of such a connection cannot be understated. Not only is the MOND relationship of $V_{inf}^4 = MGa_0$ directly reflected in the bTFR, but the zero point of the bTFR also gives a direct measurement of the constant a_0. This realization serves as the foundation for a large fraction of MOND research today.

The bTFR remains one of the most well-established methods of analysis for the dark matter paradigm. Astrophysicists on either side of the aisle use the bTFR to dive further into studying mass distributions of galaxies and their impact on their kinematics. Addressing the dark matter paradigm via the bTFR has been done in a multitude of ways. For McGaugh and his colleagues, it was decided that smaller, high-quality galaxy samples were the best method of analysis. As such, the database known as Spitzer Photometry and Accurate Rotation Curves (SPARC) was created. This sample is a "database of 175 late-type galaxies (spirals and irregulars) with Spitzer photometry at 3.6 μm (tracing the stellar mass distribution) and high-quality HI+Hα rotation curves (tracing the gravitational potential out to large radii)" (Lelli 2020). Though small in number, the sample spans a large range of stellar masses, surface brightnesses, morphological types, and gas fractions. The high quality of this dataset makes it a perfect candidate to address the dark matter paradigm.

Although Spitzer provided a solid start, the SPARC team was limited to pointed observations of galaxies with good rotation curves. Now that Spitzer has been deactivated, there is a need for this team and others to gather data with new rotation curves constantly coming into publication. My analysis directly addresses this issue, introducing data from the WISE Space Telescope as a means of extending the bTFR for hundreds of new galaxies with well-known rotation curves. The end goal of this project is to continue building on the techniques pioneered by the SPARC team and the Spitzer telescope. A transition from Spitzer to WISE data will provide new avenues for investigation into galaxy kinematics; something that is desperately needed as tensions continue to rise in this era of the dark matter paradigm.

Chapter 2: Methods

Launched in 2003, the Spitzer Space Telescope was the third NASA space telescope dedicated to infrared astronomy. Equipped with an infrared camera operating on four wavelengths (3.6, 4.5, 5.8, and 8 μm), an infrared spectrograph, and a multi-band imaging photometer, Spitzer was wildly successful. The telescope officially retired in 2020, but not without providing an abundance of important information to the scientific community. NASA archives today host a vast set of clear galaxy images in the infrared thanks to Spitzer. The telescope was not without limitations, however. Despite its vast applications, Spitzer imaging used pointed observations, meaning that the telescope would point at individual objects for a certain amount of time to capture their images. While this did allow for its images to be spectacularly detailed, the number of images it could capture was limited. This limitation carried over to the SPARC dataset, begging the question of if there is a way to acquire additional data for new galaxies with the same level of quality. Thanks to another infrared space telescope, this is now possible.

Despite no longer being active, the influence of Spitzer continues as a result of NASA archives. All NASA missions require that data obtained from these missions be archived and made available to users. The Infrared Science Archive (IRSA) contains all imaging information of both the Spitzer and WISE (see below) space telescopes. Users enter the coordinates of the galaxy of interest and can then download compressed "postage" stamps sub-images. The headers of the images contain all information concerning the instrumental calibration of the images and their characteristics. Additional celestial information on the same spot in the sky can be retrieved from the NASA Extragalactic Database (NED).

The Wide-field Infrared Survey Explorer (WISE) was launched by NASA in 2009 as part of their Explorers Program. In contrast with Spitzer, WISE conducted a series of all-sky surveys during its initial run. The overall goal was to survey 99% of the sky in the infrared, passing each section a minimum of 8 times to ensure the quality of the images. This was done using a 40 cm infrared camera, surveying in 3.4, 4.6, 12, and 22 μm wavelengths. Since both WISE and Spitzer surveyed galaxies near the 3.6 μm wavelength, there is an opportunity to include images from both telescopes in the SPARC analysis, expanding the sample considerably.

Motivations for imaging in the near-infrared originate from a variety of reasons. Most prominently, there is less extinction both internally and externally in the infrared. Extinction refers to the reduction in the brightness of objects in space as a result of their light passing through interstellar and intergalactic dust and gas. This is often a problem for astronomers as the distortion caused by extinction can alter observed properties of objects in space such as their luminosities, colors, and distances. Not only must astronomers account for the dust and gas of distant objects, but looking at these objects requires that they account for the dust and gas in our own Galaxy. Additional noise in Earth's atmosphere makes observations of galaxies nearly impossible on the ground. Hence, WISE and Spitzer being *space* telescopes is of great significance. Considering that extragalactic astronomy is contingent on the accuracy of these measurements, reducing the effects of extinction is vital. Additionally, the lack of scatter produces smoother morphology imaging, allowing for more accurate photometry of galaxies. This also opens up the opportunity to better understand the properties and characteristics of interstellar and intergalactic dust, which in turn allows for a better distinction between what is part of a galaxy and what is part of the background. The background value, known as the "sky value" refers to the brightness of the background sky in a given observation. Knowing this value

is extremely important as knowing true astronomical observations of a galaxy (such as luminosity, color, and distance) requires that the background value be removed. Thus, the more accurate this value, the less uncertain the observations. When imaging in the infrared, the sky value is near zero, removing further uncertainty that would occur under different wavelengths. High-quality images produced via infrared observations make up the SPARC database, providing increased motivation to use this database for my analysis.

Once downloaded, these archived images can be used to find the total magnitude of a galaxy. Doing so requires that the images first be "cleaned". This essentially refers to removing artifacts and objects in the background and foreground of the image. IRSA images are compressed into Flexible Image Transport System (FITS) format files common to all astronomical software. Typical images are 1500 by 1500 pixels in size with 0.6 arc seconds (arcsecs) per pixel for Spitzer compared to the 1.25 arcsecs per pixel for WISE data. Since the resolution element for WISE is a factor of 2 smaller than Spitzer, there is a larger point spread function for the WISE data of two spiral galaxies NGC 3198 and NGC 4559 as pictured below in **Figure 1.**.

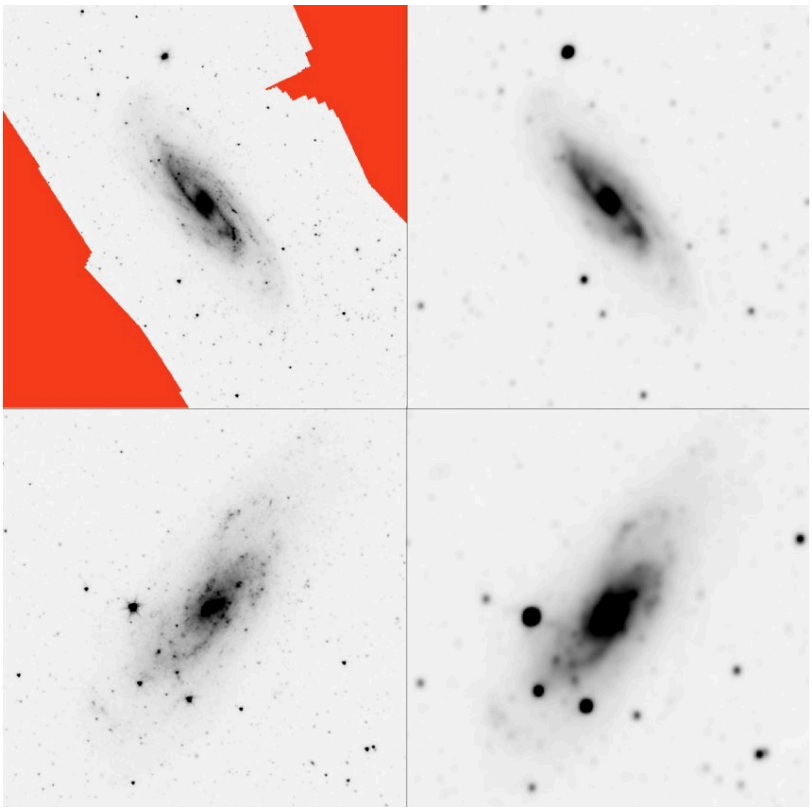

Figure 1. Two spiral galaxies from the WISE bTFR sample, NGC3198 (top) and NGC459 (bottom). The Spitzer archive 3.6μm images with 0.6 arcsecs/pixel are on the left. WISE W1 (3.4μm) 1.25 arcsecs/pixel images are on the right. Note the same morphological features (bulge, spiral arms, star-forming regions) are found in both images. Also note the poorer resolution of the WISE images compared to Spitzer (0.9 arcsec PSF for Spitzer compared to 2.5 arcsec for WISE).

This means that while in-flight processing has improved the resolution of WISE data from 2.5 arcsecs to 1.8 arcsecs, the image quality is still inferior to that of Spitzer. It should be noted, however, that this discrepancy is negligible, as the total aperture sizes of galaxies are measured in arcmins. This can be seen in the above figures when looking at foreground stars. There is a difference in the resolution, with the WISE image being "fuzzier" than its Spitzer counterpart. Despite this, however, the same features can be clearly identified in both images. Once the cleaning process was completed, we were able to add up the total light of the galaxies to produce their curves of growth and a total magnitude despite the difference in resolution; both essential elements to creating an accurate bTFR.

Adding up the total light can be done in a myriad of different ways. For this analysis, the technique used was based on a paper using Spitzer photometry (Schombert et al, 2019). This consisted of superimposing concentric ellipses around the galaxy using a least squares moment algorithm. Ellipses are a good representation of the shapes of galaxies as stars in galaxies orbit in ellipses as found by Kepler and Newton. The sizes of the ellipses can be checked via the galaxy's curve of growth which relates the total luminosity of a galaxy and the radius of the region from which this light is emitting. Typically, the curve of growth increases rapidly at first, eventually leveling off asymptotically as the radius increases. This is due to the expectation that the relationship between the total luminosity of a galaxy and its radius follows that of a power law. An eventual stabilization of this curve indicated that we had reached an accurate total luminosity. The curve of growth needs to be as flat as possible to ensure an accurate measurement of the total magnitude. To this extent, we were able to identify clear foreground objects (such as stars and galaxies) that could interfere with the curve of growth and were subsequently removed. These so-called "masked" regions were then replaced with interpolated regions nearby. Thus, the galaxy contained no holes despite the removal of foreground/background objects.

Despite the amount of effort that went into cleaning these datasets, the error produced from the aforementioned photometry and M/L models (see below) made up less than 5% of the error in this analysis. The largest source of error for the SPARC database originates in the distance (Lelli et al, 2019). In part, this is because a vast majority of distances in extragalactic astronomy are obtained through the use of Hubble's law with the calibration to the expansion rate of the Universe (H_0). The observed Doppler velocity of galaxies (redshift) is not interpreted by motion, but instead as the raw expansion of the Universe as a function of time under this framework. Locally, we can use this expansion rate to deduce distance through the use of a linear

relation between observed redshift and distance (in parsecs). This relation is known as Hubble's law ($V = H_0D$) where the observed or flow velocity is divided by Hubble's constant to deduce distance. A massive dataset has been compiled by the CosmicFlow project, containing galaxy redshifts from which flow velocities for my sample are extracted and divided using $H_0 = 75$ km/s/Mpc (Kourkchi et al, 2022). It is not uncommon to find a 20% error associated with these datasets, lending to the uncertainty in distance. To account for this, a subset of the SPARC dataset was used to construct a core bTFR using galaxies with redshift-independent distances. Redshift occurs as a result of the fact that our universe is constantly expanding. As the light from objects moving away from our point of view travels through space, it is shifted towards longer wavelengths, essentially "reddening" the light. While redshift has been used to calculate the distance to galaxies via Hubble's Law, this can be an unreliable method as the observed velocity can be easily influenced by the gravitational pull of nearby objects. This serves as the motivation behind redshift-independent galaxies, which are free from the Doppler effect (or redshift) of their light.

At this point, redshift-independent measurements are now found using the relationship $m-M = 5\log D-5$. To get an accurate distance (D), we first need accurate measurements of the flux of the galaxy (m) and its absolute luminosity (M). Historically, there are three objects/phenomena in the Universe that astronomy has a strong understanding of the underlying behavior through pure stellar physics. These include variable stars (i.e., Cepheid), red giant star evolution (i.e., TRGB), and core-collapse or carbon detonation supernova (i.e., SN II and Ia). These classic distance indicators are free from the uncertainties of the Hubble flow, minimizing the amount of error. Such low uncertainties lend an explanation for the motivation behind using these methods in my initial plot.

Cepheid stars are the first well-understood object commonly used for distance measurements. These stars pulsate in a harmonic fashion that is proportional to their luminosity. If you measure the period of pulsation, you can deduce their absolute luminosity. The second method of analysis (TRGB method) uses the fact that all stars exhaust the hydrogen fuel in their cores, which causes them to evolve into red giant branch stars (RGB). As the helium in their cores begins to burn, their maximum luminosity is set by their core mass. Since the core mass is fairly constant for all old RGB stars, this results in a "plateau" when one measures the color-luminosity of a bunch of stars known as the tip of the RGB. This has a known luminosity that can be measured from great distances, making it an excellent tool. A final technique uses the explosive end-life of a star (supernova) to measure distance through luminosity. The resulting luminosity of a supernova (SN) is given by a known percentage of the stars' mass converted into energy (think $E = mc^2$) and produces a standard candle such that if one detects an SN, a comparison between the luminosity you observe and its standard value will determine its distance (Turner 2022).

All three methods allow for the deduction of an accurate distance measurement as distance makes up the difference between the two luminosity measurements (apparent vs absolute). Additionally, the three methods have been checked for their accuracy via direct geometric methods such as parallax or proper motion. While some debate remains amongst astronomers regarding calibrating numbers, the results carry uncertainties of only 2% to 5% (Anand et al. 2021). This is a vast improvement as compared to alternative methods such as the bTFR. As such, I have only used galaxies with well-established distances using at least one of these methods (listed in **Table 1**) for my first plot: the WISE bTFR.

Table 1. SPARC Cepheids/TRGB Calibrating Galaxies

Galaxy	W1 (Vega mags)	3.6 (Vega mags)	D (Mpc)	Method
D631-7	11.853±0.08	11.694±0.05	7.87	TRGB
DDO154	10.481±0.07	12.177±0.05	4.04	TRGB
DDO161	11.747±0.07	11.442±0.05	6.03	TRGB
DDO168	11.182±0.07	11.756±0.05	4.25	TRGB
ESO563-G021	8.671±0.05	8.529±0.04	86.70	SN
IC2574	9.909±0.05	9.710±0.04	3.89	TRGB
NGC0024	8.788±0.05	8.667±0.04	7.67	TRGB
NGC0055	8.788±0.05	8.788±0.04	1.89	Cepheid
NGC0247	6.904±0.03	5.983±0.03	3.41	Cepheid
NGC0253	3.166±0.03	3.359±0.01	3.56	TRGB
NGC0300	5.780±0.03	5.780±0.02	1.91	Cepheid
NGC0891	5.511±0.03	5.343±0.02	9.12	TRGB
NGC0925	...	4.603±0.02	8.91	Cepheid
NGC1365	5.005±0.02	5.909±0.02	17.70	Cepheid
NGC1705	10.340±0.08	10.236±0.05	5.51	TRGB
NGC2366	10.720±0.08	10.612±0.05	3.34	Cepheid
NGC2403	5.743±0.03	5.541±0.03	3.18	Cepheid
NGC2541	10.240±0.03	9.405±0.05	11.50	Cepheid
NGC2683	6.149±0.03	6.029±0.03	8.59	TRGB
NGC2841	5.928±0.03	5.809±0.03	14.60	Cepheid
NGC2915	9.587±0.07	9.471±0.04	4.29	TRGB
NGC2976	7.248±0.06	7.081±0.03	3.63	TRGB
NGC3031	8.618±0.12	3.555±0.03	3.61	Cepheid
NGC3109	13.184±0.09	13.447±0.05	1.30	Cepheid
NGC3198	7.722±0.06	7.571±0.03	13.40	Cepheid
NGC3319	10.215±0.03	9.051±0.05	13.00	Cepheid
NGC3351	6.004±0.01	6.410±0.03	10.40	Cepheid
NGC3370	7.955±0.02	8.957±0.03	26.10	Cepheid
NGC3621	5.916±0.02	6.121±0.02	6.72	Cepheid
NGC3627	5.516±0.03	5.512±0.02	9.03	Cepheid
NGC3741	13.064±0.09	12.752±0.06	3.23	TRGB

Table 1 *continued on next page*

Table 1 *(continued)*

Galaxy	W1 (Vega mags)	3.6 (Vega mags)	D (Mpc)	Method
NGC3953	6.841±0.04	6.678±0.02	18.79	SN
NGC3972	9.332±0.06	9.187±0.04	20.80	Cepheid
NGC3992	6.869±0.04	6.765±0.03	22.70	SN
NGC4088	7.156±0.04	6.987±0.02	10.86	SN
NGC4214	7.911±0.04	7.990±0.03	2.93	TRGB
NGC4244	...	7.428±0.03	4.61	TRGB
NGC4258	5.831±0.02	5.241±0.02	7.31	Cepheid
NGC4414	5.966±0.02	6.639±0.02	17.80	Cepheid
NGC4535	7.577±0.02	6.919±0.02	16.10	Cepheid
NGC4536	5.889±0.01	7.113±0.02	14.60	Cepheid
NGC4559	...	7.120±0.03	8.43	TRGB
NGC4605	8.162±0.02	7.403±0.03	5.54	TRGB
NGC4639	7.382±0.02	8.537±0.02	22.00	Cepheid
NGC4725	5.999±0.02	6.122±0.02	12.50	Cepheid
NGC5005	6.329±0.03	6.292±0.03	18.37	TRGB
NGC5055	5.341±0.03	5.186±0.02	8.87	TRGB
NGC5584	9.868±0.05	9.033±0.03	22.40	Cepheid
NGC5907	6.429±0.03	6.338±0.02	17.10	TRGB
NGC6503	7.111±0.04	6.975±0.02	6.25	TRGB
NGC6946	4.940±0.03	4.629±0.02	6.72	TRGB
NGC7331	5.737±0.03	5.566±0.02	13.90	Cepheid
NGC7793	8.574±0.06	6.456±0.03	3.58	Cepheid
NGC7814	6.951±0.03	6.883±0.02	14.39	TRGB
UGC01281	10.906±0.08	10.745±0.05	5.27	TRGB
UGC05721	10.733±0.08	10.549±0.05	10.05	TRGB
UGC07151	9.267±0.07	9.161±0.04	4.61	TRGB
UGC07524	8.886±0.07	12.793±0.05	4.61	TRGB
UGC08286	9.837±0.07	9.714±0.03	6.49	TRGB
UGC08490	...	9.061±0.03	4.79	TRGB
UGCA442	...	10.862±0.04	4.37	TRGB
UGCA444	...	10.456±0.04	0.93	Cepheid

The WISE bTFR

It has been long established that the bTFR is an excellent tool for analyzing the relationship between the luminous mass of galaxies with their kinematics, the relationship stands to be improved (McGaugh & Schombert 2015). As it has been stated, there is a great deal of confidence when it comes to certain astronomical values (luminosity and M/L models). The distance to these galaxies, however, remains as a point of controversy. Additionally, the most up-to-date bTFR includes only a small sample of galaxies due to the limitations of the Spitzer Space Telescope on the number of galaxies the telescope could observe in its short lifetime. To account for this on the subset SPARC sample, 12 new galaxies with accurate rotation curves from the WISE Space Telescope have been added to an original 50 to produce a distance-accurate plot. A key part of this plot is the comparison between the Spitzer and WISE data. As such, a critical portion of this analysis involved bringing the old Spitzer bTFR galaxies into the WISE W1 color system. An equally vital procedure was to conduct accurate photometry of the galaxy sample.

To do so, I first downloaded archived galaxy images and headers that contained all instrumental information (i.e., calibration constants and coordinate map). Calibration in the headers and corrections for galactic extinction using celestial information from NED puts the WISE data on the same Vega standard system as the Spitzer data. The image frames were then cleaned for artifacts and foreground/background objects such as neighboring stars and galaxies. We then used a least squares moment analysis to fit ellipses on the galaxies. Following this, elliptical isophotes were used to fill in masked regions, calculate the galaxy's luminosity in each elliptical aperture, and create curves of growth from this information.

Since the curve of growth plots the apparent magnitude of a galaxy as a function of radius, the luminosity of the galaxy approaches an asymptotic value. As previously stated, this

allows for the extraction of the total luminosity of the galaxy after fitting this curve using rational polynomials. This value is then checked for accuracy against aperture values in existing publications. Errors are accessed by taking the error in the sky value and adding this to the Poisson noise in the apertures, although it is important to note that sky error dominates most galaxy photometry.

Ensuring the expansion of the SPARC analysis required that there be a smooth transition between the Spitzer and WISE data. The first check made on this confirmed that the mass models produced by WISE matched those produced by Spitzer. This was completed using three galaxies of different morphological types (NGC 1090, NGC 2955, and NGC 3741) and confirmed that the mass models did match the two telescopes. The new WISE filters, slightly differing from Spitzer's, also required that new M/L models be produced. Before this, however, a color comparison (W1-3.6) was made between Spitzer and WISE. By knowing the color of the galaxies in the sample, we can reduce the uncertainty in extracting the stellar mass via their luminosities. This in turn results in more accurate M/L models. Finally, to extract M/L models we look at synthetic galaxies with an assumed stellar population history made via simulation with real-world constraints imposed on the galaxy. The output produced by these synthetic galaxies is then output to observables such as color and their M/L values are read off. For astrophysical reasons, this is best done in the near-IR to minimize large discrepancies in M/L that can result from SF effects in the optical and UV ranges. Improvements such as the aforementioned, have allowed for separate corrections to be made on the bulge and disk of a galaxy. These corrections played a large role in restoring the linearity on the high mass end of the bTFR, further confirming the success of introducing WISE data to the plot (Duey et al. 2023).

More accurate M/L models and photometry have led to measurements with higher accuracy of the stellar mass of the galaxies in this analysis. To get the total baryonic mass, however, the gas mass of these same galaxies needs to be added to the stellar mass. This process is done by looking at HI fluxes and correcting this value for He abundance and molecular gas. Since hydrogen is the most abundant element in the Universe, and is well traced in the 21 cm line, measuring the flux of this provides an accurate mass value of the gas portion of a galaxy. Despite its accuracy, researchers have rightly pointed out that by correcting for He and molecular gas in this measurement, there is an improvement in the overall baryonic mass value of a galaxy (McGaugh et al. 2020). This is because about a quarter of the gas in the Universe is primordial (H and He) and some of the gas in a galaxy may take a molecular form (H_2). Both instances can be corrected for, and have been for this analysis. While these corrections may appear minuscule, they represent systematic errors that can be reduced and have been shown to improve existing correlations such as the bTFR. Once corrected, the gas mass of each galaxy can be added to its stellar mass to obtain its total baryonic mass. These values create the y-axis of the bTFR, leaving only the dynamical mass as the missing component of this analysis.

The dynamical mass is found by analyzing the characterization of a galaxy as represented by the asymptotic flat velocity outlined by Newton's law of gravity and deduced by the galaxy's rotation curve. To recap, rotation curves plot the rotational velocity of a galaxy as a function of the radius coming from the galaxy's center. Rotation curves are commonly derived by "dividing the galaxy into a series of independent rings, where the ring width is given by the spatial resolution of the observations (Lelli et al. 2019). Once completed, the average circular velocity of the galaxy (v_{flat}/v_f) can be obtained from the flat portion of the rotation curve. The criteria that define this flat region and specific methods of extracting V_{flat} can all be found in "The Baryonic

Tully–Fisher Relation for Different Velocity Definitions and Implications for Galaxy Angular Momentum" by Dr. Federico Lelli and colleagues. After defining this value, a total mass estimate of the galaxy can be made based only on the dynamics of the galaxy. It is important to note that the value of V_{flat} results directly in this "total mass" (M_{dyn} or M_{total}) estimate and resides as the measurement of interest for the x-axis of the bTFR. Dark matter enthusiasts predict that since this mass estimate involves no photometry, it includes the mass of both baryonic and non-baryonic matter (dark matter). A comparison can now be made between the dynamical mass, as deduced from V_{flat}, and the baryonic mass to test if it is baryons or dark matter that drives the kinematics of a galaxy. If we let the dynamical mass be the x-axis, this comparison makes up the present-day bTFR. The values used for both the x and y axes of the WISE bTFR calibrating plot are shown below in **Table 2**.

Table 2. SPARC Cepheids/TRGB Calibrating Galaxies

Galaxy	log V_f (km sec^{-1})	log M_{bar} ($M_\odot$)	Hubble Type
D631-7	1.76±0.03	8.699±0.050	IAm
DDO154	1.67±0.02	8.595±0.060	IB(s)m
DDO161	1.82±0.03	9.127±0.260	IB(s)m
DDO168	1.73±0.03	8.806±0.060	IBm
ESO563-G021	2.50±0.02	11.589±0.160	SAbc:
IC2574	1.82±0.04	9.262±0.060	SAB(s)m
NGC0024	2.03±0.03	9.478±0.090	SA(s)c
NGC0055	1.93±0.03	9.568±0.080	SB(s)m:
NGC0247	2.02±0.04	9.705±0.080	SAB(s)d
NGC0253	2.30±0.01	10.930±0.140	SAB(s)c
NGC0300	1.97±0.08	9.377±0.080	SA(s)d
NGC0891	2.33±0.01	10.852±0.110	SA(s)b?
NGC0925	2.06±0.01	10.230±0.100	SAB(s)d
NGC1365	2.33±0.01	11.240±0.130	(R)SBb(s)b
NGC1705	1.86±0.03	8.617±0.008	SA0-
NGC2366	1.70±0.03	9.011±0.009	IB(s)m
NGC2403	2.12±0.02	9.939±0.080	SAB(s)cd
NGC2541	2.00±0.02	10.040±0.070	SA(s)cd
NGC2683	2.19±0.03	10.579±0.110	SA(rs)b
NGC2841	2.45±0.02	11.129±0.130	SA(r)b:
NGC2915	1.92±0.04	9.040±0.060	I0
NGC2976	1.93±0.05	9.277±0.110	SAc
NGC3031	2.33±0.02	10.780±0.140	SA(s)ab
NGC3109	1.82±0.02	8.867±0.060	SB(s)m
NGC3198	2.18±0.01	10.478±0.110	SB(rs)c
NGC3319	2.05±0.04	10.060±0.080	SB(rs)cd
NGC3351	2.25±0.02	10.550±0.140	SB(r)b
NGC3370	2.18±0.01	10.400±0.130	SA(s)c
NGC3621	2.16±0.01	10.570±0.090	SA(s)d
NGC3627	2.26±0.02	10.770±0.140	SAB(s)b

Table 2 *continued on next page*

Table 2 *(continued)*

Galaxy	log V_f (km sec^{-1})	log M_{bar} ($M_\odot$)	Hubble Type
NGC3741	1.70±0.03	8.414±0.060	ImIII/BCD
NGC3953	2.34±0.02	10.915±0.160	SB(r)bc
NGC3972	2.12±0.02	10.083±0.150	SA(s)bc
NGC3992	2.38±0.02	11.119±0.130	SB(rs)bc
NGC4088	2.23±0.02	10.376±0.150	SAB(rs)bc
NGC4214	1.90±0.03	9.119±0.003	IAB(s)m
NGC4244	2.04±0.02	9.810±0.090	SA(s)cd:
NGC4258	2.30±0.01	10.760±0.130	SAB(s)bc
NGC4414	2.27±0.02	10.940±0.140	SA(rs)c?
NGC4535	2.29±0.01	10.760±0.130	SAB(s)c
NGC4536	2.21±0.03	10.620±0.130	SAB(rs)bc
NGC4559	2.08±0.02	10.171±0.270	SAB(rs)cd
NGC4605	1.94±0.02	9.640±0.130	SB(s)c
NGC4639	2.27±0.01	10.370±0.140	SAB(rs)bc
NGC4725	2.33±0.01	10.840±0.140	SAB(r)ab
NGC5005	2.42±0.04	11.087±0.130	SAB(rs)bc
NGC5055	2.25±0.03	10.878±0.100	SA(rs)bc
NGC5584	2.12±0.01	10.230±0.130	SAB(rs)cd
NGC5907	2.33±0.01	11.042±0.100	SA(s)c:
NGC6503	2.07±0.01	9.923±0.090	SA(s)cd
NGC6946	2.20±0.04	10.691±0.280	SAB(rs)cd
NGC7331	2.38±0.01	11.144±0.130	SA(s)b
NGC7793	1.98±0.04	9.750±0.110	SA(s)d
NGC7814	2.34±0.01	10.702±0.110	SA(s)ab:
UGC01281	1.74±0.03	8.764±0.060	Sdm
UGC05721	1.90±0.04	9.420±0.260	SABd?
UGC07151	1.87±0.02	8.939±0.080	SAB(s)cd?
UGC07524	1.90±0.03	9.527±0.060	SA(s)m:
UGC08286	1.92±0.01	9.163±0.060	Scd
UGC08490	1.90±0.03	9.187±0.110	SA(s)m
UGCA442	1.75±0.03	8.641±0.060	SB(s)m:
UGCA444	1.57±0.07	7.935±0.060	IB(s)m

Overall, the calibrating plot of this thesis represents a bTFR with minimized uncertainty as seen in the **Figure 2.** The y-axis, composed of the baryonic mass values of 62 redshift-independent galaxies is compared to the dynamical mass values on the x-axis of the plot. Multiple orders of magnitude require that the bTFR be a log-log plot. The linear relationship seen between the two axes was then investigated using a maximum likelihood fit as completed in previous works (Lelli et al. 2016).

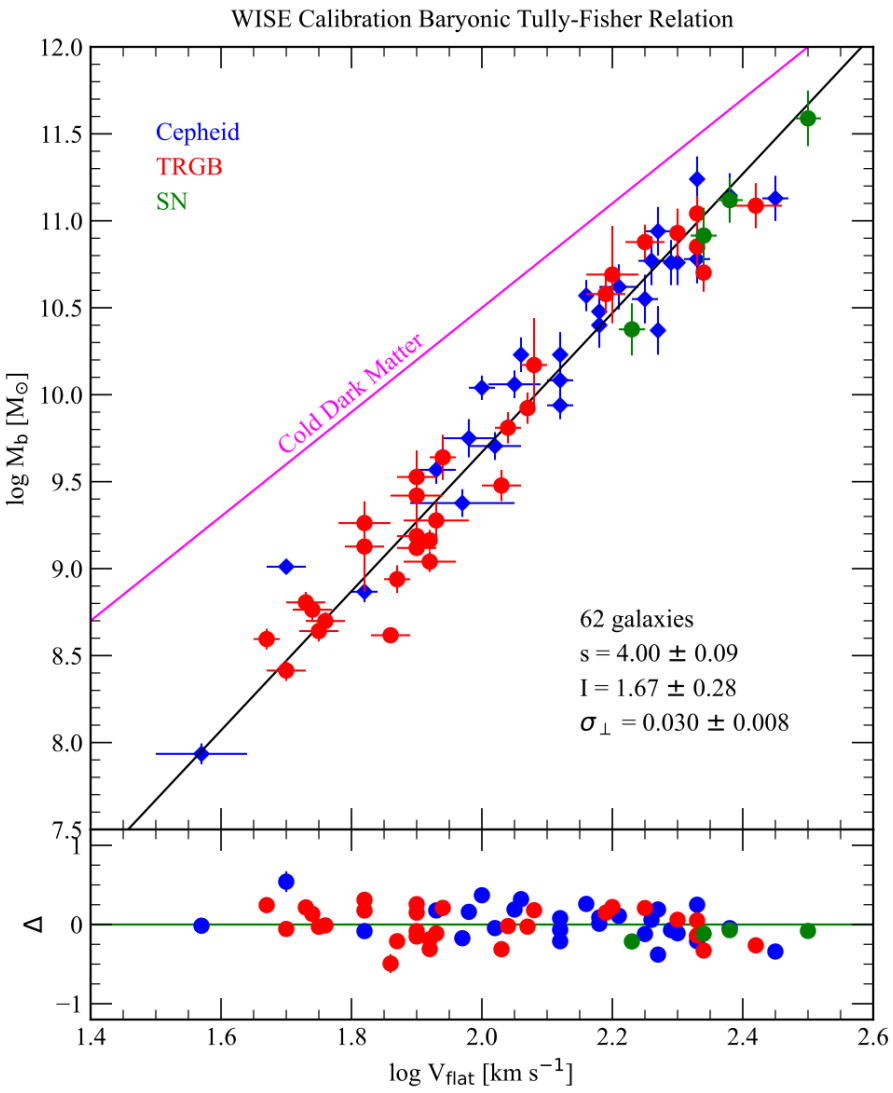

Figure 2. The bTFR diagram for 42 SPARC galaxies (diamond symbols) and 20 Ponomareva et al. (2018) disks (circular symbols) with C/TRGB distances. TRGB galaxies are marked in red, Cepheid galaxies in blue, SN distances in green. The baryonic mass is the sum of the WISE W1 luminosity converted to stellar mass (see Schombert, McGaugh & Lelli 2019) and the total gas mass (converted from HI fluxes). The rotational velocity, v_{flat} , is determined directly from HI rotation curves following the techniques outlined in Lelli et al. (2016). A maximum likelihood fit is shown compared to the CDM fit (magenta) and serves as the baseline slope and zero-point for the bTF, values of which are shown in the Figure.

The histograms below highlight the ranges of key values used to construct the WISE bTFR Calibration plot. The top left panel highlights the values of V_{flat}, ranging from about 1.6 km/s to 2.6 km/s whose individual values are listed in **Table 1**. Similarly, the top right panel gives the sample baryonic mass range from 10^6 to 10^{12} $M_\odot$ with the Hubble galaxy types included (early and late-type galaxies, spiral, and barred spiral galaxies) in the bottom left panel. The bottom right panel compares the gas mass of the galaxies (M_g) on the y-axis to their stellar mass (M_*) on a log-log plot with both measurements done in solar mass. This final plot was made to quickly demonstrate how *in general* gas-rich galaxies tend to be lower in mass. Low-mass galaxies are typically slower in acceleration, making them the perfect candidate for MOND analysis. Furthermore, this panel demonstrates that my sample has a full range of stellar and gas mass galaxies, eliminating systematic bias in the gas fraction.

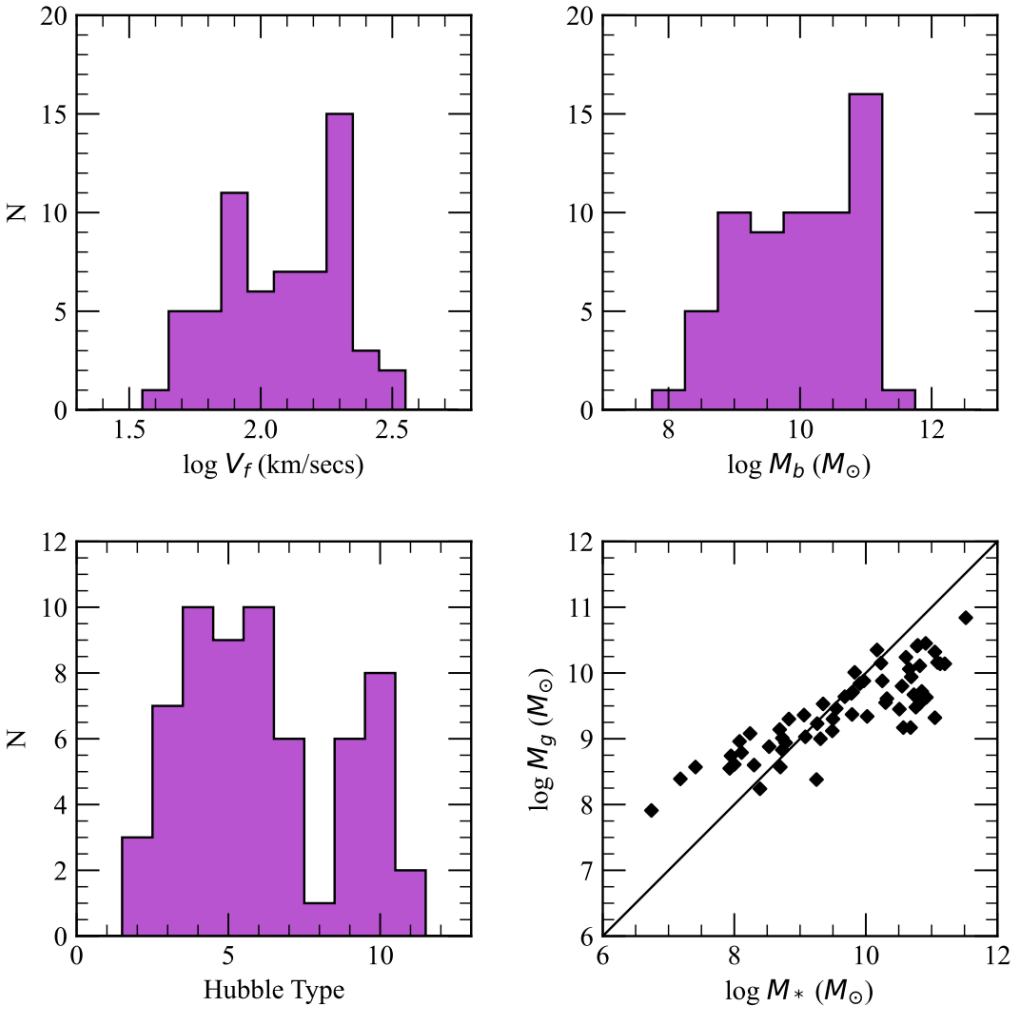

Figure 3. Histograms of the data from Table 2 for the redshift-independent WISE calibrators. Top left displays the range in v_{flat} , the asymptotic velocity. Top right displays the four orders of magnitude in total baryonic mass. Bottom left displays the range in Hubble type (where the WISE sample contains at least one example of every type of disk and dwarf galaxy). Lastly, the bottom right panel displays the known relationship between gas mass (M_g) and stellar mass ($M*$) with a line of unity shown for equal gas and stellar masses. Note that low mass galaxies are gas-rich compared to the high mass end of the bTFR.

Chapter 3: Discussion and Results

It is important to note that although the bTFR is in no way a new form of analysis to compare the relationship between the baryonic mass of a galaxy with its dynamical mass, the WISE calibration plot is another step forward in this area of research. The addition of WISE data allowed for a new development of previous models of the bTFR. Furthermore, the new data extended galaxy mass ranges on both the low and high ends, increasing the plot by an entire order of magnitude. This alone represents the vast potential WISE data holds for the bTFR. With only 12 galaxies added, vital improvements have been added that have minimized the error seen in previous calibrations. As it stands today, the calibration plot contains 42 SPARC galaxies as represented by the diamond symbols and 20 Ponomareva et al. disk galaxies represented by circular symbols (2018); all of which have been converted to the WISE photometry system. The aforementioned redshift-independent distance indicators were applied and are highlighted by the different colors on the graph. Cepheid galaxies are marked in blue, TRGB galaxies in red, and SN distances in green. A maximum likelihood fit is marked by the black line, resulting in a baseline slope and zero-point for this bTFR whose values are labeled on the graph and will be discussed in the following section.

The results from this calibration plot are astounding. Not only is the tight correlation between the baryonic mass and dynamical mass of high interest, but the value of this correlation's slope is also particularly important. Recall that MOND makes a prediction of the relationship between the asymptotic velocity and the mass of the galaxy that goes as $V_{inf}^4 = MGa_0$. This prediction has direct consequences for the bTFR as the power-law relationship predicts a slope of 4 on the bTFR. The CDM community lacks such predictive power. In the past, slope values from the bTFR using the same techniques outlined in this paper have ranged

from 3 to 3.8 (Lelli et al. 2018). The addition of new rotation curve data has continued to push this value closer to the predicted value of 4, with this value being within the uncertainty range of previous studies. When analyzed using new WISE data, however, a slope of exactly 4.00 +/- 0.09 is found as labeled on the above plot. Contrasting this, are the predictions made by CDM enthusiasts whose slope values typically range from 2 to 3 (Zwaan et al. 1995, McGaugh 2012). Under the assumption that Newton's law of gravity holds at all accelerations and that the dark matter halo dominates the mass of a galaxy (especially at large radii). This essentially follows the original predictions made by the virial theorem which states that luminosity (L) goes as $R * V^2$. Thus, when V goes as R for a rising rotation curve, then L now goes as V^3. This sort of assumption leads to a differing power-law relationship than that of MOND, and results in a predicted slope of 3 on the bTFR. Clearly, this is not the case as seen by my first plot. Instead, this has confirmed the success of transitioning from Spitzer to WISE data as seen in decreased uncertainty. A reduction of error by 50% as compared to previous works suggests that the addition of WISE data on both the high and low-mass ends of the bTFR improved the overall analysis (Schombert et al. 2022).

The significance of this low scatter cannot be understated. Just as seen in the original TF relation, there is a clear correlation between the rotational velocity of a galaxy and its baryonic mass. Once again, this is something *not* predicted by the CDM community (McGaugh 2004). Historically, there are two main competing ideas in cosmology when it comes to galaxy formation and evolution: MOND and CDM. Recall that under CDM theory, galaxies formed in a hierarchical manner. Dark matter theoretically served as the dominant gravitational influence when it came to mass distribution as smaller structures combined to eventually form the galaxies we see today. As a consequence of this, CDM also predicts that the dark matter halo of a galaxy

should range in size and shape depending on the galaxy. This would then be reflected on the bTFR through scatter in the observed velocities of the stars and gas of a galaxy. The shallow slope predicted by CDM also predicts that errors on the bTFR should propagate up. In other words, scatter on the bTFR should be smaller on the low-mass end and increase as one moves towards the high-mass end. The consistent, small amounts of scatter that are instead seen imply that baryons play a more dominant role in determining the gravitational potential of a galaxy than originally predicted by CDM. At best, this correlation is unexpected by the CDM community. Contrasting this, however, are the predictions made by MOND with the results seen by the WISE bTFR calibration plot. The residual error of 0.03 +/- 0.008 is well within the observational error of the photometry, HI flux, and distance. Considering the error exists across a vast range of galaxy types, masses, and morphologies, this is suggestive of a pure empirical law of nature. In other words, the only error in the fit of this graph is purely observational. This implies that even if the observational error were to decrease, the relationship seen on the WISE bTFR would remain unchanged. More specifically, given the velocity at the flat portion of a particular galaxy's rotation curve, one could immediately deduce the baryonic mass. There is no need to take dark matter into consideration, quite literally what you see in a galaxy is what you get in its rotational velocity and vice versa.

Cosmological Constant (a_0) from the bTFR

A final point of interest on the WISE bTFR is the intercept point on the y-axis. Under the MOND framework, where $V_{inf}^4 = MGa_0$ the y-intercept will give a value for a_0 . This value has massive implications for the MOND framework. Put simply, a_0 determines the scale at which MOND becomes important in studying galaxy motion. While a_0 is not a prediction from this framework, it is a value that can be extracted from observations. An analogous example is the

ability to get a value for G out of Newton's Law of Gravity $F = G(m_1m_2/r^2)$. Clearly, the value of G is not directly given in this formula. If one knows enough additional information, however, G can easily be derived. This same technique can be used to find a_0. Since the bTFR is in log-log space, the actual y-intercept cannot be used as it is far outside the range of values. To accommodate this, the midpoint of the graph is instead used. An exact slope of four represents the substitution of a V_{flat} and M_{bar} value near the midpoint in addition to a straight-forward calculation of a_0 from the MOND equation. Once this technique has been applied, a resulting value of 1.29 (+/- 0.05) x 10^{-10} m/s^2 is found with the uncertainty defined solely by the error in the y-intercept. This value is in agreement with past values in the range of (Banik & Zhao 2021). Considering that a_0 serves as the acceleration at which the standard Newtonian regime ends and MOND's altered laws take over, it is essential to narrow down the value of this constant. With this value, the three primary components of the WISE bTFR (slope, scatter, and zero-point) have been successfully determined. The former two observed values present serious challenges to the CDM framework. Common responses from the CDM community have consisted of 1) ignoring the existence and meaning of these values or, 2) claiming stellar physics will eventually provide the needed explanation (Famaey & McGaugh 2012). Clearly, there is a crucial need to facilitate conversation surrounding the results of this analysis and similar works.

Full SPARC bTFR

It can be stated with confidence that the WISE bTFR calibration plot was a success in terms of data quality, even with the addition of WISE data. The obvious standing limitation in this analysis is now the quantity of the sample itself. As such, the next logical step was to take the results of the calibration sample and apply this fit to the entire SPARC sample of 154 galaxies. It is important to note that this sample no longer contains only redshift-independent

galaxies. Not only are the galaxies in this new sample influenced by errors in the Hubble Flow, but their velocities are also impacted by regions of higher density and thus, greater gravitational influence (Kourkchi et al. 2022). Hence, a new method of analysis needed to be used to estimate the distances to the sample galaxies. Recall a note earlier in this paper that referred to the CosmicFlow velocity database which contains distance information for over 10,000 galaxies (Graziani et al. 2019). The researchers who put the database together did so by building density contour maps of the local Universe. Using this, they were able to estimate the peculiar velocity (difference between Hubble flow velocity and observed velocity) of the galaxies in question. The value of this flow velocity is then divided by a standard H_0 value of 75 km/s/Mpc to obtain the distance to the galaxies in question. The M_{bar} of these galaxies is then calculated from W1 luminosity and HI flux. These distance and mass values were then used for the entire SPARC sample, resulting in my second plot (**Figure 4**).

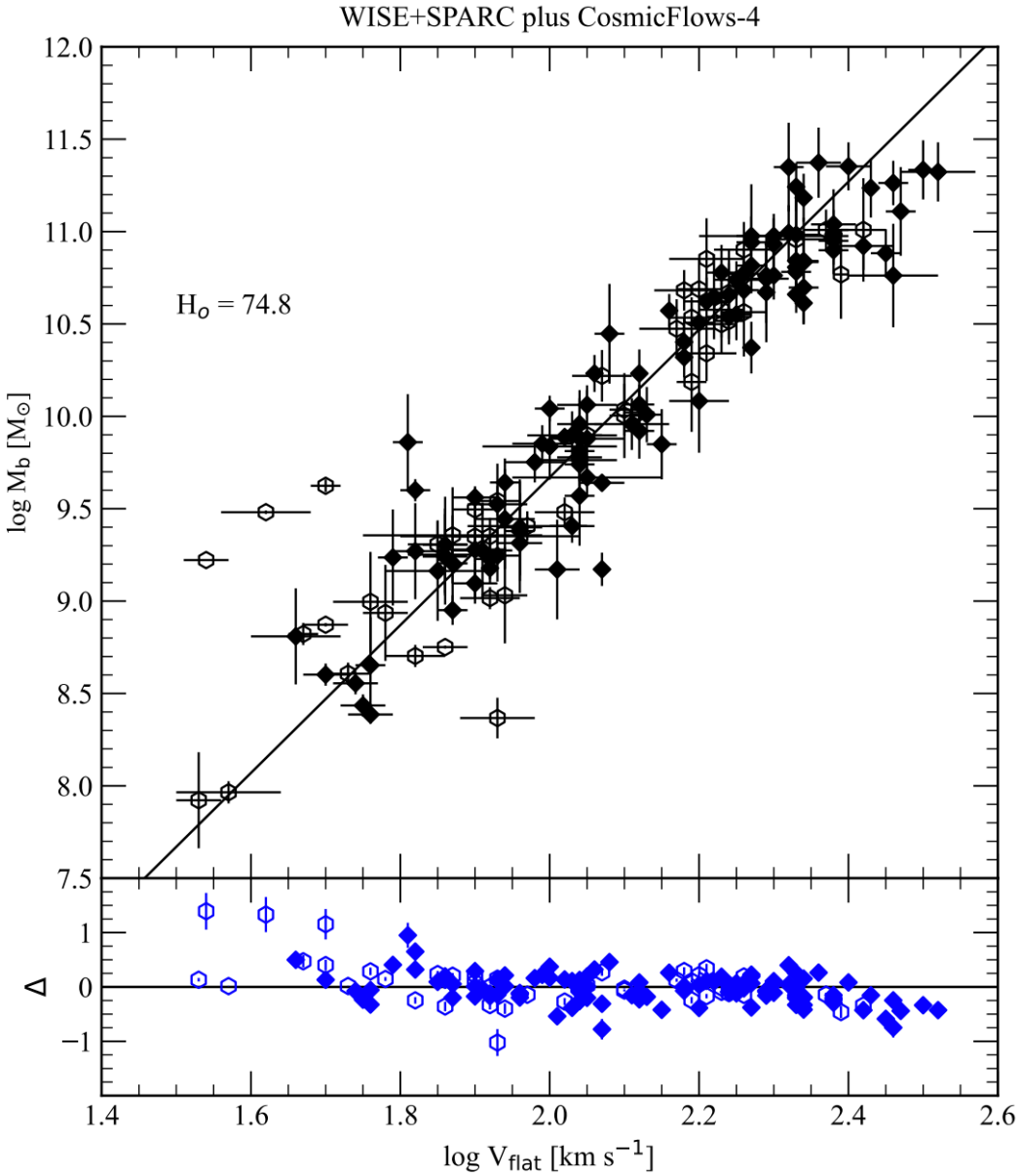

Figure 4. The bTFR for the flow SPARC galaxies, using CosmicFlows-4 velocities, with H_0 = 74.8 km s^{-1} Mpc^{-2} (top panel). The solid line is the baseline fit from Figure 1. Residuals are plotted in the bottom panel. As V_f is independent of distance, changing H_0 has the effect of increasing the baryon mass by ΔH_0 . H_0 values less than 70.5 are ruled out at the 95% confidence level.

The slope of 4.00 +/- 0.09 from the calibration plot was applied to the secondary, supplementing the need to repeat the fitting process to a less accurate sample. This is in response to the fact that the galaxies in the SPARC sample introduce new sources of noise and error. It is

important to note, however, that it is absolutely necessary to analyze the entire SPARC sample despite these new errors. Using rotation curves as the primary form of analysis has proven to be more accurate as compared to alternative forms such as HI line widths (Lelli et al. 2019). The sample size itself also aids in lowering the overall error given by individual data points. While the individual points may have more uncertainty than their redshift-independent counterparts, the sheer quantity of the data reduces this additional noise. Nevertheless, the uncertainty in the SPARC sample would negatively influence the slope of the bTFR should a completely new fit be made to the dataset. Seeing that the calibration plot was made using the best quality data, it is logical to apply this fit to the full SPARC sample instead. Using this methodology also allows for the opportunity of future projects including the extension of the bTFR using high redshift galaxies. As more galaxy rotation curves are modeled, more data points can be added to the bTFR. Thus, by performing accurate and consistent methods of examination now, future work in this area of research can be done with greater ease.

H_0 from the bTFR

Fitting the SPARC sample with the slope deduced from the calibration plot also opens another avenue of investigation. This results from the idea that one can use the relationship $V = H_0D$ to minimize the residuals from the fit to the distance-corrected SPARC data. Doing so requires taking V as an independent variable, varying instead the value of H_0. This results in a new value of distance (D). Since luminosity (L) is proportional to D^2, and we extract the baryonic mass from luminosity, a new value for this is also found. Rather than a mathematical comparison, this change can be directly measured on the bTFR. Changing H_0 results in sliding an entire axis up/down until the distance between the SPARC sample points and slope line is at a minimum. To be clear, this method is not “fitting the data” but rather reducing the residuals of

the rotational velocity with respect to the calibrating plot. Since we have established that the calibration plot represents the very best of the data sample, doing so serves as an excellent quality check. Once the velocity residuals have been minimized, a new H_0 value can be extracted. At first glance, doing so does not seem strictly necessary as H_0 is already indirectly determined by the CosmicFlow studies. This assumption is simply untrue, as there remains a great deal of debate surrounding the value of this cosmological constant. Known today as the "Hubble tension", this controversy refers to a discrepancy between two value ranges of Hubble's constant. When one uses the cosmic microwave background (CMB) as a form of measurement (in agreement with CDM frameworks) average values ranging from 65-67 km/s/Mpc are found (Di Valentino 2021). Alternatively, observing the distances and redshifts of nearby galaxies using traditional astrophysical methods instead results in a vastly different value, nearing 75 km/s/Mpc. When using the bTFR using the techniques outlined above, I found a value of 74.8 km/s/Mpc; a value that is in agreement with the latter techniques used by MOND researchers. The errors associated with this result are particularly interesting. Unlike other values presented in this thesis, the uncertainties in Hubble's constant have two primary sources. The systematic errors (sys) are due to errors in the calibrating methods and errors in the calibrating bTFR fit. My study is unique compared to other H_0 studies in that I use three calibrating distances (cepheids, TRGB, and SN) with no evidence in the bTFR that any method produces biased distances. If I consider the average of the distance scale errors, combined with the error in the zero-point of the bTFR fit, I can assign a systematic error of +/- 1.2 km/s/Mpc.

A second source of error (statistical) will result from the scatter of the SPARC galaxies using flow distances from the calibrating bTFR with a slope of four. The scatter in this is about 20% less than the original scatter in the SPARC data due to improved photometry from the

WISE data. Thus, I can assign a statistical error of +/- 0.08 km/s/Mpc. This value is in agreement with the mean value of what is referred to as "high" H_0 values using traditional astrophysical methods (Riess et al. 2020).

Outside of the Hubble tension, deducing a specific H_0 value holds significance for deriving an accurate value of a_0 from the full SPARC sample bTFR. Doing so required the repeated utilization of the relationship $V = H_0D$. In this case, we took the flow velocities as defined by the CosmicFlow database and multiplied this by the deduced H_0 value (74.8 km/s/Mpc). This results in a new distance value that in turn gives new baryonic mass (M_b) values for the SPARC galaxies. Using the relationship $V_{inf}^4 = MGa_0$, we were able to take our V_f values and divide them by the new M_b values and the gravity constant G to isolate a new value of a_0. While a value of a_0 was already found in the calibration plot, it is important to remember this was done using only 62 galaxies. The full sample contains over double this number, making for a more statistically accurate value of a_0. Further backing up this methodology is that used in previous literature. According to current researchers, the above analysis represents the simplest and most direct way to measure a_0 under the MOND framework. With that in mind, the value of a_0 from the full SPARC bTFR was found to be $1.4 * 10^{-10}$ m/s^2. Not only is this value close to the one found in the calibrating plot (again confirming the calibration plot's accuracy), but is in agreement with previous attempts (Banik & Zhao 2021). Current CDM models have no explanation for the existence of this value. There is no expectation for a constant that can be extracted from the bTFR. The existence of such a constant conjoined with the fact the MOND framework *does* predict a_0 introduces yet another empirical challenge to the CDM community. Overall, the goal of extending the bTFR was to use WISE data as the next photometric archive to derive stellar to baryonic masses. Doing so allows for a deeper investigation into the baryon-dark

matter connection being seen in this relationship. Based on the agreement between the derived values with existing literature, and the multitude of checks between the two plots, it can be said with confidence that this goal was achieved successfully.

The progress made on the bTFR through this analysis represents a major turning point for MOND. While the framework is not a fully working theory (lacking a clear relativistic extension), the predictive success remains unmatched in today's astrophysical community. It is important to note that it is nearly impossible to build a theory that is consistent with all known facts. MOND, and even the CDM theory, are not exempt from this. Nevertheless, it is equally impossible to explain the predictive successes of MOND in terms of dark matter. The values obtained from the bTFR alone (slope, scatter, a_0, and an H_0 that is inconsistent with CDM theory), have little to no explanation under a CDM framework. This is not to say that CDM is wrong, but instead to draw attention to the idea that it is clearly time to seriously consider alternative frameworks. Over fifty years have passed since CDM theory gained popularity. Yet in that time, no clear detections of dark matter have been obtained. In this same amount of time, MOND has yet to have been falsified. It is becoming increasingly clear that there is a need to not only shift our perspective but to also start examining how science in this community is being conducted.

Chapter 4: Conclusion

Consistent and continuously improving results from MOND have made it impossible for the astrophysics community to ignore the alternative framework. Willful ignorance will always be an option, but this does nothing to change the fact that the predictive power of MOND continues to produce substantial explanations for the missing mass problem. Of course, it is plainly evident that MOND is in no way a complete theory. Many unanswered questions remain on both sides of the issue that seem nowhere near a distinct answer. The analysis presented in this paper may support some of the predictions made by MOND, but was not intended to solve any of these issues. Put simply, the goal of this analysis was to present evidence to ask questions, not answer them. The baryonic Tully-Fisher Relation is arguably the most fundamental tool of analysis when it comes to the relationship between the kinematics and stellar mass of a galaxy.

My study has improved the linearity of the bTFR, reduced the scatter, and asserted a specific value of a_0. The methods presented in this thesis to find the value of a_0 are specifically important. Previous work to determine a_0 has depended on looking at the relationship of expected Newtonian acceleration against the expected acceleration. More specifically, a_0 was found to be the point at which the transition from baryon dominance to dark matter dominance (V^2/R) occurred. While the value of a_0 from my own research is within the error ranges of these previous attempts, it should be noted that basing what may very well be a new cosmological constant on a deviation is not a fully accurate method. The bTFR provides a much more established avenue to determining this constant. Using the bTFR in this fashion has been done in the past, but was never the main focus of the project. Thus, my work has established a more statistically sound method of determining a_0 in addition to providing a path for future researchers to repeat this same analysis.

Taken individually, these results depict incremental improvements to an already established astrophysical relationship. The real impact is seen when considering these results together. Overall, the research presented in this thesis is a substantial leap forward in the MOND interpretation of galaxy kinematics. These results from my work on the bTFR lack context when under current CDM theory. These outcomes have, however, been consistently expected under a MOND framework. The community in this area of research has been publishing innovative and progressive solutions for the missing mass problem *without* dark matter for decades. Refusing to attend to these results can be interpreted as conducting poor science. It is true that even false theories can generate correct predictions. This has been a common theme throughout history, and remains prudent today. In an age where science denialism has become an increasingly popular default for many, it becomes all the more important to constantly be aware of how we as scientists conduct ourselves and our research. Separating science from pseudoscience comes down to the ability to falsify. While this is not necessarily a straightforward process, it is nevertheless vital to do so and becomes "the responsibility of the scientist to adopt a methodology that maintains falsifiability" (Merritt 2020). The CDM model as it stands today is nearly impossible to falsify. While this framework succeeds in the reproduction of astrophysical characteristics such as galaxy rotation curves, this is done using a litany of free parameters whose constant adjustments allow for this success. Additionally, it can and should be argued that reproducing reality does not in fact mean the origins of this reproduction are themselves real. MOND by no means is a complete theory, but stands above the CDM model when it comes to the scientific method. Milgrom began with a series of predictions, then looked to see if the evidence was supportive or contradictory. In doing so, Milgrom was able to ensure that MOND can easily be falsified. Since this has yet to happen in the fifty years since the framework's

inception, it begs the question as to why this framework continues to be largely ignored by the astrophysics community. In general, MOND has a great deal more explanatory power for the observed galaxy kinematics than it is generally given credit for. The increase of linearity as mass ranges continue to increase, a continued narrowing of the slope, and the deduction of an a_0 value are all serious results produced by this framework that certainly deserve consideration by the CDM community. It is up to the individual to step back and question the lack of consistency in the CDM framework and consider that the missing mass problem may be better answered outside the kinematic realm. The results produced from this analysis and similar works are all indicative of the progressive and innovative qualities the MOND framework possesses. Such qualities are pinnacle characteristics of promising research programs. MOND has always possessed such attributes, which is encouraging and suggests that a new era of understanding gravitational physics may be emerging.

Future Directions

The future directions of this project hope to continue addressing this issue and will continue to investigate this problem using the standard scientific method. Given the name "SPARC 2.0", this upcoming project will focus on expanding the sample size of the bTFR. Data from both the Atacama Large Millimeter/sub-millimeter Array (ALMA) and the James Webb Space Telescope (JWST) will be the primary focus of this investigation. The intent of this expansion is to evaluate how the bTFR evolves with redshift and to expand the current mass range. More specifically, the goal is to expand the SPARC database by a factor of ~5 by covering the database of 21 cm data for around 1000 galaxies of all masses and morphological types provided by the radio observational community. In this new dataset, higher and lower mass galaxies and those with low surface brightness will be specifically addressed. A critical

component to this extension is the stellar mass determinations given by the all-sky WISE archive of which this poster presents the preliminary results for the first calibration techniques from pointed Spitzer observations to the all-sky WISE archive. When combined with the gas mass from HI surveys, the total baryonic mass of this new extensive sample can be realized.

Bibliography

Alcock, C., Allsman, R. A., Alves, D. R., et al. 2000, ApJ, 542, 281.

Aprile, E., Abe, K., Maouloud, S. A., et al. 2023, arXiv:2304.10931.

Banik, I. & Zhao, H. 2022, Symmetry, 14, 1331. doi:10.3390/sym14071331

Blumenthal, G. R. 1983, Science, 221, 1281.

Begeman, K. G., Broeils, A. H., & Sanders, R. H. 1991, MNRAS, 249, 523.

de Blok, W. J. G. 2010, Advances in Astronomy, 2010, 789293. doi:10.1155/2010/789293

de Vaucouleurs, G. 1960, ApJ, 131, 585. doi:10.1086/146871

Di Valentino, E., Anchordoqui, L. A., Akarsu, O., et al. 2021, Astroparticle Physics, 131, 102605. ¨ doi:10.1016/j.astropartphys.2021.102605

Duey, F., Tosi, S., & Schombert, J. 2023, Seattle AAS Meeting #241

Faber, S. M. & Gallagher, J. S. 1979, ARA&A, 17, 135.

Gnedin, N. Y. 2012, ApJ, 754, 113

Graziani, R., Courtois, H. M., Lavaux, G., et al. 2019, MNRAS, 488, 5438.

Jungman, G. 1996, Dark Matter in Cosmology Quantam Measurements Experimental Gravitation, 33

Kourkchi, E., Tully, R. B., Courtois, H. M., et al. 2022, MNRAS, 511, 6160.

Lelli, F., McGaugh, S. S., Schombert, J. M., et al. 2019, MNRAS, 484, 3267.

Lelli, F. 2022, Nature Astronomy, 6, 35.

Lelli, F., McGaugh, S. S., & Schombert, J. M. 2017, VizieR Online Data Catalog, J/AJ/152/157
Li, P., Lelli, F., McGaugh, S., et al. 2019, ApJ, 886, L11. doi:10.3847/2041-8213/ab53e6
McGaugh, S. S., Schombert, J. M., Bothun, G. D., et al. 2000, ApJ, 533, L99.

Lelli, F. “SPARC (Spitzer Photometry and Accurate Rotation Curves).” *SPARC*, 23 May 2020, astroweb.cwru.edu/SPARC/.

McGaugh, S. S. 2004, ApJ, 611, 26.

McGaugh, S. S. 2012, AJ, 143, 40.

McGaugh, S. 2014, Galaxies, 2, 601.

McGaugh, S. S. & Schombert, J. M. 2015, ApJ, 802, 18.

McGaugh, S. 2020, Galaxies, 8, 35. McGaugh, S. S., Lelli, F., & Schombert, J. M. 2020, Research Notes of the American Astronomical Society, 4, 45.

Merritt, D. 2020, A Philosophical Approach to MOND: Assessing the Milgromian Research Program in Cosmology, by David Merritt. Cambridge Series in History and Philosophy of Physics and Astronomy. ISBN: 9781108492690, 2020

Milgrom, M. 1983, ApJ, 270, 365.

"NASA/IPAC Extragalactic Database." *One-Line Query Entry*, ned.ipac.caltech.edu/.

Navarro, J. F., Ludlow, A., Springel, V., et al. 2010, MNRAS, 402, 21.

Olive, K. A. 2016, arXiv:1604.07336.

Ostriker, J. P. & Peebles, P. J. E. 1973, ApJ, 186, 467.

Peebles, P. J. E. 1982, Astrophysical Cosmology Proceedings, 165

Ponomareva, A. A., Verheijen, M. A. W., Papastergis, E., et al. 2018, MNRAS, 474, 4366.

Riess, A. G., Yuan, W., Casertano, S., et al. 2020, ApJ, 896, L43.

Rubin, V. C., Ford, W. K., & Thonnard, N. 1980, ApJ, 238, 471.

Sancisi, R. 2004, Dark Matter in Galaxies, 220, 233.

Scarpa, R. 2006, First Crisis in Cosmology Conference, 822, 253.

Schombert, J., McGaugh, S., & Lelli, F. 2020, AJ, 160, 71.

Tully, R. B. & Fisher, J. R. 1977, A&A, 54, 661

White, S. D. M. & Rees, M. J. 1978, MNRAS, 183, 341.

White, S. D. M., Frenk, C. S., & Davis, M. 1983, ApJ, 274, L1.

Zwaan, M. A., van der Hulst, J. M., de Blok, W. J. G., et al. 1995, MNRAS, 273, L35.

Zwicky, F. 1933, Helvetica Physica Acta, 6, 110.